Polymer Chemistry

PAPER

View Article Online
View Journal | View Issue

Cite this: *Polym. Chem.*, 2014, **5**, 1313

On the effect of using RAFT and FRP for the bulk synthesis of acrylic and methacrylic molecularly imprinted polymers†

Carlo Gonzato,*[a] Pamela Pasetto,[b] Fahmi Bedoui,[c] Pierre-Emmanuel Mazeran[c] and Karsten Haupt*[a]

Molecularly imprinted polymers (MIPs) are synthetic polymeric receptors, capable of specifically binding a target molecule, just like a biological antibody. There has been a recent trend to improve the properties of these materials by using modern methods of controlled radical polymerization (CRPs) for their synthesis. Despite the recognized advantages associated with their "living character", the effect of the "controlled nature" has still to be clearly demonstrated. This is far from obvious as the high amounts of short cross-linkers normally used for their synthesis complicate the formation of homogeneous polymer networks. In order to gain more insights into the potential benefits for the binding properties of MIPs resulting from the use of CRPs, the imprinting of a model target (*S*-propranolol) has been used to compare reversible addition–fragmentation chain transfer polymerisation (RAFT) and free-radical polymerisation (FRP) on acrylic and methacrylic matrices. While most MIPs are based on methacrylates, we used acrylates as a "difficult imprinting matrix" for comparison. In fact, the absence of the methyl groups in their polymer back-bone reduces their entanglement, resulting in a more flexible network. This renders the material more difficult to imprint, and at the same time makes it easier to evaluate the effects of RAFT polymerization and FRP on structural parameters and thus binding properties. Moreover, we also progressively reduced the amount of cross-linking in order to explore the effects of RAFT and FRP on a wider range of scaffold rigidities. Although MIPs are normally highly cross-linked, some recent emerging applications require lower degrees of cross-linking. Binding experiments, SEM, BET, DMA, swelling and nanoindentation analyses revealed that RAFT is effective in promoting the synthesis of more homogeneous networks compared to FRP, even at very high cross-linker contents, which results in higher target affinities, especially in the case of acrylates.

Received 6th September 2013
Accepted 23rd October 2013

DOI: 10.1039/c3py01246h

www.rsc.org/polymers

Introduction

Molecularly imprinted polymers (MIPs) are synthetic, biomimetic receptors for target molecules.[1,2] Their affinity and selectivity are often on a par with those expressed by natural systems such as antibodies and enzymes.[3] Due to these characteristics they are commonly termed "antibody mimics" or "plastic antibodies".[4] To obtain these properties, three-dimensional binding sites are created upon a templating process at the molecular level, which involves the copolymerization of interacting (functional) and cross-linking monomers around a template molecule to form a cast-like shell.[5,6] Upon removal of the template, cavities that are complementary to the template in shape, size and position of functional groups are revealed, so that the material can specifically recognize and bind its target. In contrast to the random copolymerization occurring in the absence of any templating molecule, the interaction between the template and the functional monomers (*e.g.* covalent or non-covalent depending on the adopted imprinting strategy) locally induces a non-statistical copolymerization, so that "regions" able to express specific and selective binding to the target molecule are generated. MIPs are usually synthesized using high amounts of short cross-linkers (*e.g.* by radical polymerization with ethyleneglycol dimethacrylate EGDMA, trimethylolpropane trimethacrylate TRIM, or by polycondensation with tetraethyl orthosilicate TEOS). Such a high amount of cross-linkers has been historically found to be the most convenient way for giving the three-dimensional binding sites the stability that natural systems achieve *via* an elegant and complex network of hydrogen bonds, electrostatic interactions, hydrophilic and hydrophobic forces. However, such high levels of cross-linker that produce high fidelity binding sites also

[a]*UMR CNRS 6022, Compiègne University of Technology, BP 20529, 60205 Compiègne, France. E-mail: karsten.haupt@utc.fr*

[b]*UCO2M – UMR 6011, University of Maine, 72085 Le Mans, France*

[c]*Laboratoire Roberval UMR 7337, Compiègne University of Technology, BP 20529, 60205 Compiègne, France*

† Electronic supplementary information (ESI) available. See DOI: 10.1039/c3py01246h

make MIPs difficult to study from a structural point of view; MIPs are insoluble networks, with gelation and/or phase separation occurring quite early during their polymerization process. Moreover, the interactions between the template and the functional monomers introduce additional "cross-links". These characteristics make the study of molecularly imprinted materials considerably more complicated than that of poorly cross-linked matrices or, in general, of networks synthesized by homopolymerization of long bridged cross-linkers. At the same time, these features also make it difficult to evaluate and rationalize the impact of new polymerization techniques, in particular in the case of MIPs synthesized by free-radical polymerization (FRP) the use of controlled/living radical polymerization methods (CRPs).

Due to a series of inherent advantages (*i.e.* versatility, easy setup, wide range of available monomers and experimental conditions) the great majority of MIPs has been (and still is) synthesized by free-radical polymerization.[7] However, upon the introduction of the modern CRP techniques during the 80's and the 90's, *e.g.* NMP,[8] ATRP[9,10] and RAFT/MADIX,[11–14] the perspectives in the field of radical polymerization have dramatically changed, and characteristics until then exclusive to ionic polymerisations (*i.e.* low PDI polymers and living character) have become available to radical processes. Over the last decade, CRPs have been applied to the synthesis of MIPs as well,[7,15,16] showing extremely important results, especially in the synthesis of composite systems and hierarchical structures,[17–22] thanks to their living character that allows for restarting the polymerization for the synthesis of consecutive blocks. Although it may seem obvious that a more controlled synthesis of MIPs may result in a better quality, more homogeneous polymer network and thus in better binding properties, the impact of the controlled nature of CRPs on the binding and structural properties of MIPs has been difficult to evaluate and elucidate, due to the abovementioned high level of cross-linkers used in MIP copolymerization. Thus, the correct understanding of how CRPs impact the structure, as well as the binding properties of MIPs, is important for choosing between CRPs and FRP (when living character is not required). Despite some recent interesting contributions,[23–26] systematic investigations on this subject are still lacking. Several studies have been published over the years on the synthesis of cross-linked networks by CRPs, often including a comparison with equivalent FRP matrices.[27–32] However, as mentioned above, such studies have been focused on formulations containing rather low amounts of short cross-linkers, or on high amounts of long bridged species (*e.g.* oligo ethylene glycol dimethacrylate), which considerably differ from MIPs. In these cases, the controlled character of CRPs resulted in more homogenous networks than FRP, with a generally improved distribution of cross-linking points resulting in increased swelling, narrower glass transition temperature regions, and increased cross-linking corresponding to gelation. An interesting comparison of Yu *et al.*,[31] focusing on the RAFT, ATRP and FRP copolymerisation of oligo(ethylene glycol) methyl ether and oligo(ethylene glycol) dimethacrylate, showed for instance that the autoacceleration (Trommsdorf effect) is postponed when RAFT and ATRP are used, and, most importantly, the application of these techniques results in an overlap of microgelation and macrogelation points; in contrast to FRP, where rapid *intra*molecular reactions between propagating radicals and pendant double bonds in vicinity are favored, thus generating various cyclizations and densely cross-linked domains (microgels), the uniform distribution of reactive species in RAFT and ATRP minimizes the microgel formation by facilitating *inter*molecular cross-linking. The closer onsets of micro and macrogelation in RAFT and ATRP also suggest that a different gelation mechanism is involved. In another relevant contribution, Armes and co-workers[33] demonstrated that a branched system ($M_w/M_n = 36.1$) synthesized by RAFT copolymerization of methyl methacrylate with a disulfide-based dimethacrylate, simply consisted, upon cleavage of the branching agent, of statistically linked, near-monodisperse, primary chains ($M_w/M_n = 1.24$), thus further demonstrating the ability of such polymerization processes to move toward an ideal distribution of cross-linking points.

In the present work, we analyzed the impact of RAFT and FRP on the synthesis of polymers imprinted against a model template: S-propranolol. Although MIPs are normally based on methacrylic polymers due to their rigid nature that facilitates the obtention of stable three-dimensional binding sites, this study has been developed by considering, in addition, acrylic polymers as a model for a "difficult" imprinting matrix (in fact, the absence of the methyl groups in their polymer backbone reduces the entanglement, which makes the network more flexible). Similarly, the effect of using RAFT and FRP has also been studied on MIPs having a low degree of cross-linking. While this gave us in particular the opportunity to compare RAFT and FRP and to visualize the impact of each polymerization technique on these matrices, MIP scaffolds combining both flexibility and recognition properties are also interesting *per se*, as they have become relevant for some emerging applications such as controlled drug delivery[25] and sensing.[34] We correlate equilibrium binding properties and structural characteristics based on FT-IR, SEM, BET, DMA, swelling measurements and nanoindentation analyses.

Experimental section

Material

(*S*)-Propranolol hydrochloride, [^{3}H]-(*S*)-propranolol, methacrylic acid (MAA), methyl methacrylate (MMA), methyl acrylate (MA), neopentyl glycol diacrylate (NPGDA) and 4-cyano-4-[(dodecylsulfanylthiocarbonyl)sulfanyl]pentanoic acid (m-TTCA) were from Sigma-Aldrich. Acrylic acid (AA) was from Acros Organics. Neopentyl glycol dimethacrylate was from Sartomer, USA. 2-(Dodecylthiocarbonothioylthio)-2-methylpropanoic acid (a-TTCA) was from Orica Consumer Products. 2,2′-Azobis-(2,4-dimethylvaleronitrile) (Vazo-52) was from DuPont Chemicals. Toluene, methanol and acetic acid (GPR rectapur) were from VWR. THF (reagent grade) was from Fisher Chemical. (*S*)-Propranolol hydrochloride was converted into the free base by extraction from a sodium carbonate solution at pH 9 into chloroform. All chemicals were used as received.

RAFT synthesis of P(M)MA

In a two-necked round bottom flask sealed with a rubber septum, toluene (40 mL), the RAFT agent a-TTCA (for MA) or m-TTCA (for MMA) (0.546 mmol), MA or MMA (120.01 mmol) and Vazo-52 (0.109 mmol) were mixed together and nitrogen purged for 20 min at room temperature. The reaction mixtures were then immersed in an oil bath heated at 60 °C and 0.5 mL samples were periodically withdrawn to gravimetrically measure the conversion. After complete drying, the raw polymer from each sample was dissolved in THF for size exclusion chromatography analysis.

RAFT synthesis of *S*-propranolol-imprinted acrylic polymers using a-TTCA

In a 4 mL glass vial sealed with a screw cap and a silicone septum a-TTCA (3.41×10^{-5} mol), *S*-propanolol (4.87×10^{-5} mol), AA (3.90×10^{-4} mol), NPGDA (1.95×10^{-3} mol) and the radical initiator Vazo-52 (6.82×10^{-6} mol) were dissolved in 1 mL of toluene. Analogous recipes containing reduced cross-linker percentages were prepared by progressively decreasing the molar amount of NPGDA in the standard formulation to 75%, 50%, 30% and 15%. The simultaneous addition of a non-functional monounsaturated monomer (MA) allowed for maintaining the total double bond concentration. The resulting mixtures were purged with nitrogen for 2 min at RT and then heated using an oil bath preheated at 60 °C. After 2 hours, the reactions were stopped by cooling in an ice bath. The polymers were then crushed and manually ground. The template was extracted by three incubations in methanol/acetic acid (9 : 1), followed by three incubations in methanol for 1 hour each. After incubation, particles were collected by centrifugation at 10 000 rpm for 15 min. The imprinted polymers were dried under vacuum and stored at room temperature until use. Non-imprinted control polymers (NIPs) were synthesized under identical conditions in the absence of the template molecule.

RAFT synthesis of *S*-propranolol imprinted methacrylic polymers using m-TTCA

In a 4 mL glass vial sealed with a screw cap and a silicone septum m-TTCA (3.41×10^{-5} mol), *S*-propanolol (4.87×10^{-5} mol), MAA (3.90×10^{-4} mol), NPGDMA (1.95×10^{-3} mol) and the radical initiator Vazo-52 (6.82×10^{-6} mol) were dissolved in 1 mL of toluene. As above, analogous recipes containing a reduced cross-linker percentage were prepared by progressively decreasing the amount of NPGDMA by simultaneous addition of monounsaturated MMA. The resulting mixtures were purged with nitrogen for 2 min at RT and then heated overnight in an oil bath thermostatted at 60 °C. The polymers were crushed and manually ground. The template was washed out using the previously described procedure. NIPs were synthesized under identical conditions in the absence of the template molecule.

Synthesis of *S*-propranolol imprinted acrylic and methacrylic polymers under free-radical conditions

Imprinted polymers were synthesized according to the previously described recipes, except that the RAFT agents were omitted. The Vazo-52 amount was increased by a factor of 2.5 (1.70×10^{-5} mol), in order to provide the same number of active radicals. The polymerizations were performed overnight. As above, NIPs were synthesized by omitting the template molecule.

Analytical instrumentation and characterisation techniques

Average molecular weights (M_n) and molecular weight distributions (M_w/M_n) of the linear polymers P(M)MA were measured using Size Exclusion Chromatography (SEC) on a system equipped with a SpectraSYSTEM AS1000 autosampler, with a guard column (Polymer Laboratories, PL gel 5 μm Guard, 50 × 7.5 mm) followed by two columns (Polymer Laboratories, 2 PL gel 5 μm MIXED-D columns, 2 × 300 × 7.5 mm), with a SpectraSYSTEM RI-150 and a SpectraSYSTEM UV2000 detectors. The eluent used was THF at a flow rate of 1 mL min^{-1} at 35 °C. Polystyrene standards (580 to 483 000 g mol^{-1}) were used to calibrate the SEC.

Glass transition temperature (T_g) measurements were recorded on a Metravib 150+, by applying a sinusoidal (1 Hz) 0.05% deformation on cylindrical specimens. The samples were heated in air from 25 to 200 °C, with a ramping rate of 2°C min^{-1}.

Nanoindentation measurements on polymer discs were done with an Agilent 200 nanoindentor, by using a Berkovitch type tip, working in a CSM method (from 2000 to 3000 nm).

BET surface area measurements were performed using a Quantachrome Nova 1000e instrument with dinitrogen as an adsorbate at 77 K. Samples were degassed under vacuum at room temperature for at least 15 h prior to analysis.

FT-IR spectra were recorded using a Thermo Nicolet 6700 instrument with a MCT-B detector in ATR mode (from 4000 cm^{-1} to 675 cm^{-1}, resolution 4 cm^{-1}, 120 scans).

For estimating the molecular weight between cross-linking points (M_c), weighed amounts of polymer, crushed using zirconia beads (2.8 mm diameter) in a Precellys 24 (Bertin technologies), were incubated in NMR tubes with an excess of toluene for a week. After removal of the exceeding solvent, the volume fraction (Q) of the polymer in the swollen mass was calculated according to eqn (1) from Li *et al.*[35] (by assuming the polymers being equivalent respectively to PMMA and PMA):

$$Q = \frac{w_s d_r}{w_g d_s} \quad (1)$$

where w_s (g) represents the weight of solvent, w_g (g) the weight of gel, d_s (g mL^{-1}) the density of solvent and d_r (g mL^{-1}) the density of the polymer. The Q value (averaged on three measurements) was then used for estimating the weight-average molecular weight between cross-links (M_c) (g mol^{-1}) according to eqn (2):[35]

$$M_c = \frac{2 d_r V_1}{V_p^{5/3}(1 - 2\chi)} \quad (2)$$

where V_1 (mL mol^{-1}) is the molar volume of the solvent, V_p is the volume fraction of the polymer in the swollen mass and χ is the Flory–Huggins interaction parameter. eqn (3) gives the

relationship between V_p and Q. See Table S1† for details on calculations.

$$V_p = \frac{1}{1+Q} \quad (3)$$

In radioligand binding experiments, different amounts of MIP and NIP, ranging from 1 to 7 mg were prepared in a series of Eppendorf tubes. 1 mL of 0.647 nM [^{3}H]-*S*-propranolol solution in toluene + 1% acetic (v/v) acid was then added to each tube and the resulting dispersions were incubated overnight on a rocking table at RT. After centrifugation at 17 500 rpm for 30 min, a 0.5 mL aliquot of the supernatant was transferred from each tube into scintillation vials containing 3 mL of scintillation fluid (Beckman Coulter). The concentration of the free radioligand was measured with a liquid scintillation counter (Beckman LS-6000 IC).

Results and discussion

In this study, the well-established, non-covalent imprinting of *S*-propranolol using methacrylic acid as the interacting monomer[36–38] has been chosen as a model system for comparing the effect of RAFT and FRP on the binding properties and structural parameters of bulk imprinted scaffolds. To make our analysis more comprehensive, and to correlate binding and structural features to the specific polymerization process easier, acrylic formulations have also been studied. The physical entanglement of the polymer back-bone in acrylics is much less important and the stress built up in the network can mainly be related to the covalent cross-linking. By keeping this in mind, we used acrylics as a means for demonstrating, understanding and rationalizing the effects of RAFT and FRP on MIPs. The monomers copolymerized in this study are illustrated in Fig. 1. In order to cover a wide range of cross-linking degrees, actually useful for establishing some systematic tendencies characterizing the effects of RAFT and FRP, the cross-linker content has been progressively reduced by replacing one mole of NPGD(M)A with two moles of M(M)A, thus keeping the total number of double bonds present in the system constant. This strategy, previously reported by Mosbach and co-workers,[39] allowed the study of the effect of the cross-linking degree while having a negligible impact on the matrix polarity, thus preventing any additional non-specific binding of the target propranolol. We were thus able to study the effect of RAFT and FRP on poorly cross-linked matrices, which are gaining importance in the MIP field as they are required by some emerging applications (*e.g.* controlled drug release in imprinted hydrogels and chemical sensing[25,34]). Before focusing on the effect of RAFT and FRP on *S*-propranolol MIPs, we have performed some preliminary tests on linear PMA and PMMA to elucidate how the absence of any stirring (a condition normally applied to the synthesis of MIPs) might impact on the control of the RAFT process. As can be seen in Fig. S1 (ESI†), M_n increases linearly with conversion for both linear polymers, and PDIs remain lower than 1.3, thus indicating in both cases a good degree of control; for PMA, the control is kept for conversions up to 70%, afterwards some transfer reaction probably occurs, leveling off M_n and increasing PDIs. Nevertheless, up to 70%, PMA polymerization is well controlled. It is also interesting to observe how PMA polymerizes much faster than PMMA: some 70% conversion is reached in just 2 hours for PMA, while it takes almost 24 hours for PMMA. This observation, which is consistent with the different propagation rate constants reported for MA and MMA, ($k_p = 2090$ L mol^{-1} s^{-1} and $k_p = 515$ L mol^{-1} s^{-1}, respectively, at 60 °C)[40] has to be taken into account when comparing acrylic and methacrylic scaffolds: if a reduced entanglement of the polymer back-bone is important for reducing the total constraints undergone by the growing macroradicals during the

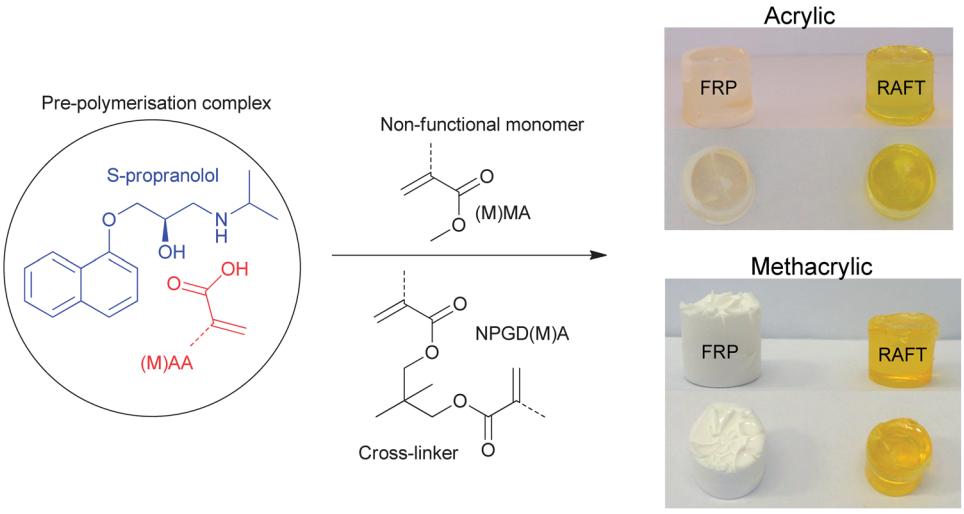

Fig. 1 Reaction scheme of the synthesis of FRP and RAFT bulk MIPs. The first step consists of mixing the template (blue) with the functional monomer (red) in order to create the so-called "pre-polymerisation complex" (black circle). Such complex then reacts with a cross-linker (NPGD(M)A) and eventually with a non-interacting monomer (M(M)A). Resulting FRP and RAFT specimens are depicted on the right as acrylics and methacrylics. (M) indicates a methacrylate monomer, while the methyl group in the relative chemical structures is represented by a dashed line.

propagation step, a lower polymerization rate is convenient, since it favors relaxation phenomena affording the development of more homogeneous structures. According to the above results, we set a polymerization time for RAFT acrylics of just 2 h (*i.e.* the time required by PMA for reaching 70% conversion), while we kept an overnight period for RAFT methacrylics. Moreover, for FRPs the amount of Vazo-52 was increased to 1.70×10^{-5} mol, in order to provide the same number of active radicals as in RAFTs. In fact, in the case of RAFT polymerisation, the number of propagating species is assumed to be equal to the number of RAFT agents. To compare the polymers synthesised with the same number of propagating species, for FRP a molar amount of ABDV corresponding to half the molar amount of the RAFT agent was then used (taking into account that each ABDV generates two radicals). We now synthesized a series of MIPs and the corresponding non-imprinted reference polymers (NIPs) based on acrylic or methacrylic monomers, with a varying degree of cross-linking (see formulations in Table 1), using both RAFT polymerization and FRP. The ability of the MIPs to bind their target propranolol was studied through equilibrium radioligand binding assays with [^{3}H]propranolol. Fig. 2 and S2 (see ESI†) show equilibrium binding isotherms fitted by using the Langmuir model for a series of RAFT and FRP MIPs. It is interesting to observe how an imprinting effect (IF) can be clearly achieved for formulations up to A/M30. Similarly, it is important to notice that methacrylic MIPs express higher affinities than the corresponding acrylic MIPs (*i.e.* lower K_{50} values, Table 1). This prominent difference can mainly be related to the entanglement effect generated in the polymer backbone by the methyl groups in methacrylates. As stated above, this contribution is additional to the effect induced by the covalent cross-linking, and it considerably affects and improves the overall rigidity, thus favoring the development of stable high affinity binding sites. This "methyl effect" is also consistent with the observation that, upon reduction of the nominal cross-linking content, the expected affinity loss is less pronounced for methacrylates compared to acrylates (*e.g.* the affinities of M30s are similar to those of A75s, the moles of the cross-linker in the former being only 40% the moles in the latter, see Table 1). When focusing on the polymerization technique, it can be observed that RAFT generates higher (slightly higher for methacrylates) affinity MIPs compared to FRP, and this improvement tends to be more evident as the nominal cross-linking content decreases down to A/M50; for very low cross-linking contents, the binding properties of RAFT and FRP MIPs tend to level off, with M15 showing no-imprinting effect.

It might be objected in considering the above results that the RAFT agent bearing a carboxylic group, this may interact with the template molecule, altering the comparison between RAFT and FRP in favour of the former, and being responsible for some increased affinity. However, analysis of the binding affinities for reference particles (NIPs) clearly shows that RAFT and FRP have an identical behaviour, thus excluding any contribution arising from the carboxylic group of RAFT agents. This important characteristic seems to be peculiar to CRPs, as an analogous result has also been reported by Byrne and co-workers for the imprinting of diclofenac sodium and ethyl adenine-9-acetate by a photo-iniferter approach.[25] In our case, however, we also found that the improvement obtainable with RAFT is related to the apparent degree of cross-linking: by decreasing this parameter to half (*i.e.* from A/M100 to A/M50) the binding difference between RAFT and FRP progressively increases on MIPs, while no variations can be observed on NIPs (see Table 1). This particular aspect suggests that RAFT can in part compensate the decrease in rigidity corresponding to the reduction of the apparent cross-linking degree. Nonetheless, the fact that this positive effect can only be observed on MIPs indicates that the different polymerization mechanism induced by RAFT directly deals with the imprinting step, and it boosts it over conventional FRP. Based on these results, we now focused our attention on the structural parameters responsible for the improved binding properties generated by RAFT, and among the different formulations, we concentrated our attention on the antipode A/M50 and A/M100 matrices, wherein RAFT gives respectively its highest and lowest effect on MIPs over FRP. For

Table 1 Feeding molar ratios used for the synthesis of acrylic (A) and methacrylic (M) imprinted (MIPs) and non-imprinted reference (NIPs) polymers; apparent binding affinities (K_{50}) and RAFT/FRP binding ratios for MIPs and corresponding reference polymer NIPs

	Molar ratios							
Polymer label	Template	(M)AA	M(M)A	NPGD(M)A	K_{50} RAFT[a] (mg mL^{-1})	K_{50} FRP[a] (mg mL^{-1})	MIP $_{RAFT/FRP}$[b]	NIP $_{RAFT/FRP}$[b]
A100	1	8	0	40	1.29	1.79	1.14	0.98
M100	1	8	0	40	0.21	0.88	0.98	~0
A75	1	8	20	30	3.14	3.13	1.22	0.94
M75	1	8	20	30	0.24	0.30	1.15	0.24
A50	1	8	40	20	10.28	14.44	1.33	0.93
M50	1	8	40	20	1.16	1.83	1.37	0.95
A30	1	8	56	12	—	—	1.27	1.26
M30	1	8	56	12	3.57	4.27	1.12	0.86
A15	1	8	68	6	—	—	1.10	1.13
M15	1	8	68	6	—	—	—	—

[a] Obtained by fitting Langmuir isotherms using a GraphPad Prism (one site-specific binding mode). [b] Calculated based on the amount of bound template at concentrations of 1 mg mL^{-1} and 7 mg mL^{-1} for methacrylates and acrylates, respectively.

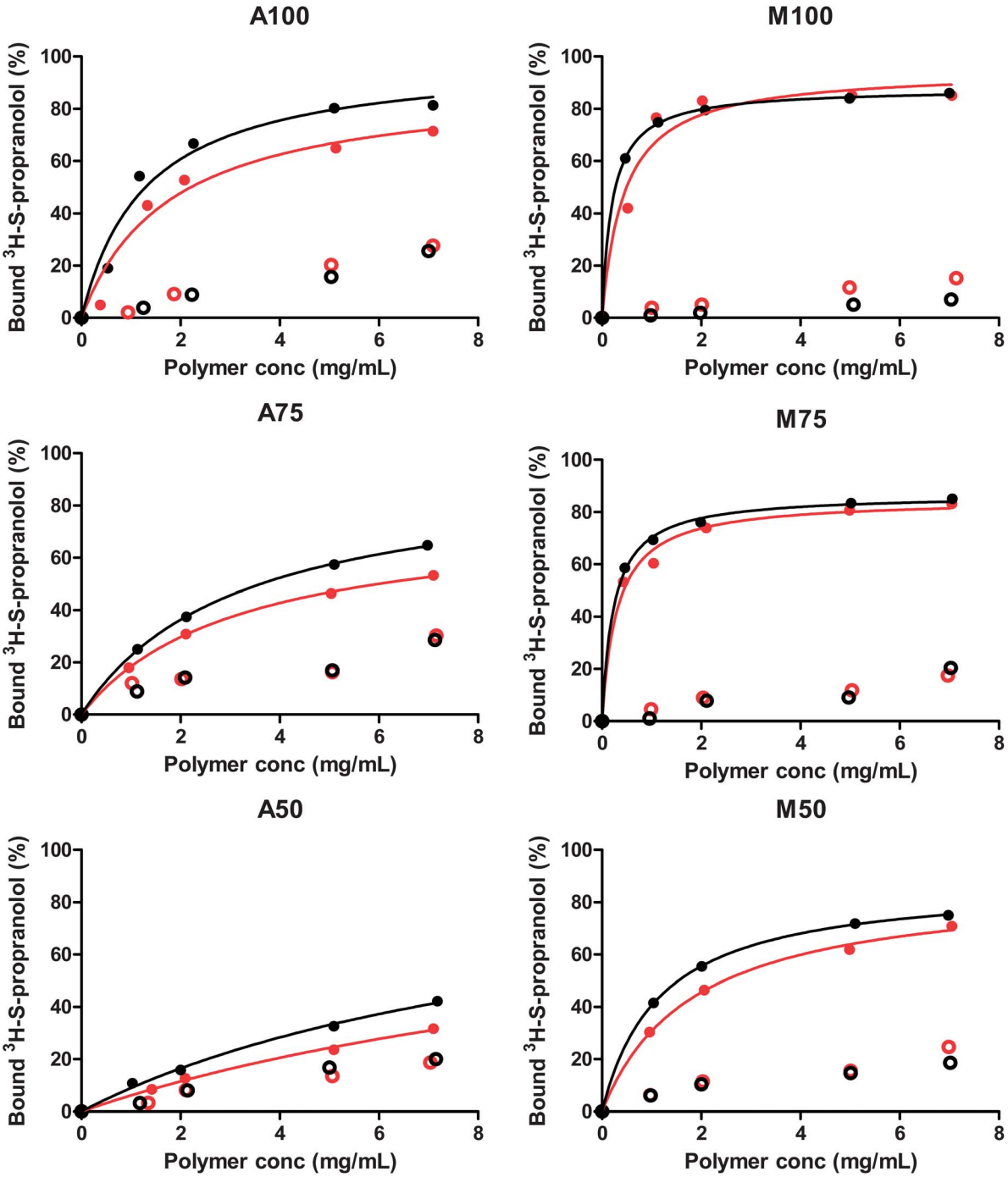

Fig. 2 Equilibrium binding experiments for acrylic (A) and methacrylic (M) matrices obtained under RAFT (black) and free-radical (red) conditions. Imprinted polymers are indicated by filled symbols, non-imprinted, control polymers by empty symbols. For A/M30 and A/M15 see ESI, Fig. S2.†

this study to be a more general one, disregarding the imprinting template, we purposely analyzed references particles (NIPs) rather than MIPs.

The first macroscopic difference that we observed was the aspect of polymer monoliths synthesized by RAFT and FRP: while RAFT samples were always perfectly transparent (MIPs, as well as NIPs), FRP resulted in white or opaque materials (Fig. 1). This important difference suggested, for FRP, the presence of spatial inhomogeneities affecting the refractive index, which may be reasonably related to the presence of microdomains able to scatter light (*e.g.* ref. 41). The transparency of RAFTs would then suggest that such inhomogeneities are not present, or at least to a considerably lesser extent.[28] To get a clearer picture of the different microstructures generated by the different polymerization methods, we analyzed the samples by SEM. As shown in Fig. 3, the structures generated by RAFT and FRP are considerably different and their aspects are markedly dependent on the relative cross-linker (CL) content. When

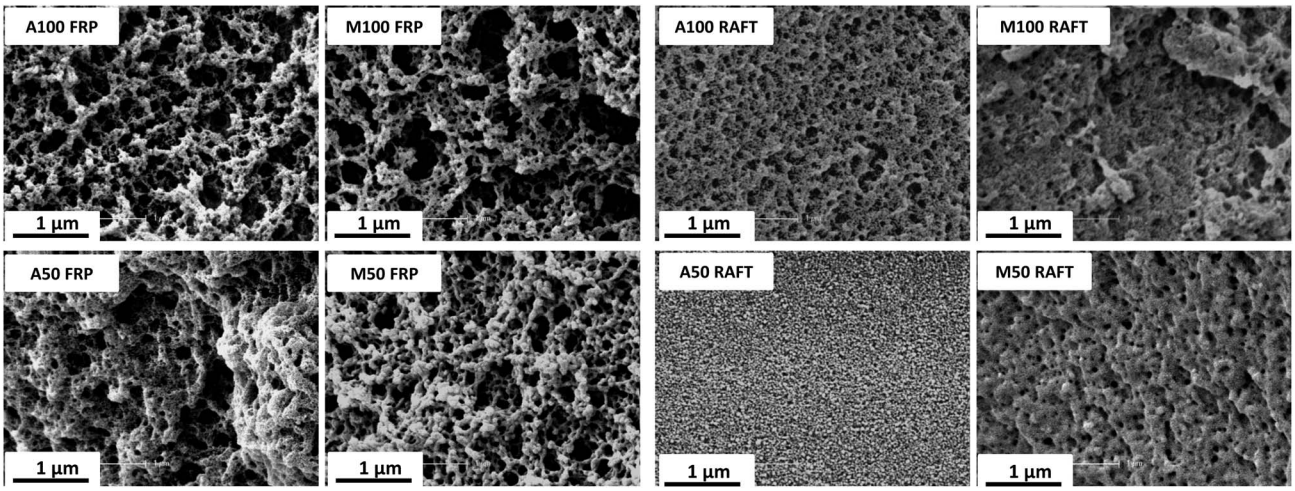

Fig. 3 SEM images of A/M100s and A/M50s reference, control polymers (NIPs) synthesized by free-radical (FRP) and RAFT polymerisation.

focusing on methacrylates, RAFT results in very compact, collapsed networks, which show little dependence on the CL content. Conversely to RAFT, FRP generates in M100 a highly porous structure, as commonly reported for free-radical MIPs synthesized in toluene (*i.e.* the porogenic solvent). FRP polymers also show a dependence on the CL content as the porous structure in M50 is less extended than the one in M100 and it seems to be affected by an increased degree of collapse. For acrylates, collapsing phenomena are more pronounced, and this may be related to the absence of the methyl group in their polymer back-bone; as for methacrylates, structures obtained by using RAFT and FRP showed marked differences. For A100, porous structures were obtained in both cases (using RAFT as well as FRP), but upon reduction of the CL content to A50, the RAFT matrix became extremely compact while an appreciable porosity was still observed for FRP, although an evident collapse has occurred. Based on the above SEM micrographs, it is evident that RAFT leads to a more efficient collapse upon shrinking. This may be the result of a more homogeneous inner structure (generated upon the use of controlled RAFT conditions) and in particular of a more homogenous distribution of cross-linking points compared to FRP, as previously suggested.[30,32] To quantitatively support these assumptions, we analyzed the porous structures by BET and swelling measurements. A preliminary FT-IR analysis on the double bond conversion in A/M100 and A/M50 networks revealed that conversions are in the range of 60% to 75% (Tables 2 and S2, see SI†), with FRP generally affording higher conversions, especially on A/M100s (*i.e.* RAFT $\leq$ 15% FRP). These values are important since they indicate that our comparison on RAFT and FRP involved scaffolds having similar degrees of double bond conversions. Therefore, any difference measured for the above matrices (*e.g.* the increased affinity of RAFT MIPs) can be reasonably associated with a different balance between *intra*- and *inter*-molecular cross-linking, as well as to physical entanglement phenomena on acrylates and methacrylates. BET analyses (Table 2) proved our SEM-based hypotheses to be consistent; M100 RAFT and M50 RAFT showed an identical surface area (*i.e.* 4 $m^2\ g^{-1}$), thus indicating that the efficient collapse is not dependent on the apparent degree of cross-linking. On the other hand, FRP proved to be very sensitive to this parameter: the high surface area obtained for M100 FRP (*i.e.* 185 $m^2\ g^{-1}$) markedly dropped in M50 (*i.e.* 40 $m^2\ g^{-1}$), although in both cases values considerably higher than for the equivalent RAFT polymers were obtained. Our results were also consistent with previous work of Sasaki *et al.* who reported very different surface areas upon the use of ATRP and FRP in the covalent imprinting of bisphenol-A.[42] Nevertheless, our values are in sharp contrast with some recent results published by Zhang and co-workers,[26] who focused on the bulk imprinting of propranolol and bisphenol-A by RAFT and FRP. In that case, the authors reported that both RAFT and FRP generated surface areas of about 250 and 400 $m^2\ g^{-1}$ on, respectively, P(MAA-*co*-EGDMA) and P(VP-*co*-EGDMA) NIPs, with MIP values being very close to NIPs. However, it has to be observed that Zhang and co-workers used a different cross-linker (*i.e.* ethylene glycol dimethacrylate instead of NPGD(M)A) and a lower molar ratio RAFT agent/radical initiator (2 instead of 5). Our BET analyses on acrylates, revealed a trend similar to methacrylates, with surface

Table 2 Double bond conversion, surface areas and molecular weights between cross-linking points (M_c) for A/M100s and A/M50s synthesized by RAFT and FRP

Sample	Conversion[a]	Surface area[b] ($m^2\ g^{-1}$)	M_c[c] ($g\ mol^{-1}$)
A100 RAFT	62%	16.3	~2200
A100 FRP	71%	37.3	~2100
M100 RAFT	62%	4.4	~900
M100 FRP	73%	184.5	~800
A50 RAFT	60%	0.4	~1800
A50 FRP	57%	1.5	~1500
M50 RAFT	67%	4.6	~900
M50 FRP	68%	39.7	~900

[a] Double bond conversion measured by FT-IR. [b] Obtained by BET analysis using dinitrogen at 77 K as adsorbate. [c] Based on swelling measurements (eqn (2), Experimental section).

areas lower for RAFT than for FRP, but with an important difference: in this case both techniques generate lower areas upon reduction of the CL content. In particular it is interesting to observe how the surface area for RAFT polymers decreased about 40 times when moving from A100 to A50, while only of 25 times in the case of the corresponding FRP polymer. Swelling measurements in toluene (*i.e.* the polymerization solvent) have then been used to roughly estimate the molecular weight between the cross-linking points (M_c; see Table S1 in ESI† for details on calculations). The results listed in Table 2 indicate that the polymerization technique has a negligible effect on methacrylates; unfortunately M_c is the average molecular weight and its value does not give any information about the real molecular weight distribution. RAFT and FRP afforded similar results on both M100 and M50. On the other hand, acrylates exhibited higher M_cs, which are dependent on both the CL content and the polymerization technique. On A100, M_c for RAFT and FRP is very similar, with their values being more than twice that of the corresponding M100. However, on A50 M_c decreased instead of increasing, with RAFT affording a higher value compared to FRP. Such an unexpected decrease can be explained by assuming that in A50 the *inter*-molecular cross-linking is actually more pronounced compared to A100, and this may be associated with a reduced stress on the growing macro-radicals resulting upon the introduction of MA, reducing *intra*-molecular cyclisation. The values in Table 2 also account for the different template affinities exhibited by acrylic and methacrylic MIPs, and in particular for the effect of decreasing the nominal CL content. The lower M_c in methacrylates is consistent with more rigid structures which, in turn, are able to express higher affinity binding sites. On the other hand, the relative stability of M_c upon reduction of CL to half in methacrylates is also consistent with their ability to maintain good template affinities. Similarly, the higher M_c estimated for acrylates can be related to their lower affinity compared to methacrylates, especially upon decreasing the CL content. However, despite the fact that the lengths between cross-linking points (M_c) in RAFT polymers are in most cases similar to, or higher than the equivalent FRP polymers, RAFT has shown to favor the formation of imprinted networks possessing higher affinities compared to FRP. This may be in principle related to different dispersities (also known as polydispersities) affecting the above M_c; one way for validating this hypothesis was to measure the breadth of the T_g region for RAFT and FRP networks, as reported by Yu *et al.*[32] Fig. 4 reports tan δ *versus* T measured by DMA on A50; as can be seen, the RAFT polymer has a lower T_g (50 °C instead of 66 °C) and a narrower T_g half-height breadth (23 °C instead of 31 °C) than the FRP polymer. A lower T_g is consistent with a higher M_c (and probably with a plasticizing effect arising from the long alkyl chain of the Z group in RAFTs), but the narrower half-height breadth clearly suggests that a more homogenous distribution of the cross-linking points has occurred in the RAFT polymer, as observed by Yu *et al.* on long bridged dimethacrylates networks.[32] Unfortunately, A50s were the only samples that we were able to analyse by DMA, since A/M100 as well as M50 lost their mechanical properties before reaching their T_g region (data not shown). Nevertheless, it seems reasonable to expect and generalise a similar behaviour for the remaining samples. Nanoindentation analysis on M50 discs showed for instance that the use of RAFT results in a tenfold increase in both indentation modulus (E^*) and hardness (H) compared to FRP (*i.e.* $E^*_{M50RAFT} = 3.7$ GPa, $E^*_{M50FRP} = 0.3$ GPa; $H_{M50RAFT} = 0.2$ GPa, $H_{M50FRP} = 0.01$ GPa), thus confirming that the CRP approach is also effective in improving the mechanical properties, as previously suggested by Fukuda and co-workers.[43] We could not compare this behaviour on A50s, since the free-radical polymer was so inhomogeneousthat the test could only be correctly made on the RAFT polymer (*i.e.* $E^*_{A50RAFT} = 2.5$ GPa, $H_{A50RAFT} = 0.1$ GPa). According to these results, RAFT can effectively promote the development of more homogenous structures, mainly due to a more homogenous distribution of CL points. This aspect can directly be associated with the improved match between chain propagation and chain relaxation, which has already been invoked on slightly cross-linked matrices synthesized by CRP.[28–30,32,43] This particular aspect has shown to be very important for molecularly imprinted polymers, since it allows the generation of MIPs having improved template affinity. The entire set of data, especially for RAFT polymers, also gave us the opportunity to qualitatively evaluate the 'methyl effect' in terms of physical entanglement as well as in terms of monomer reactivity. It is well known that the methyl group in methacrylates is responsible for the hyperconjugation effect which decreases their reactivity compared to acrylate monomers.[44] This explains why MMA polymerises slower than MA (see Fig. S1†). On the other hand, the methyl group is also responsible for an increased physical entanglement of the main polymer back-bone, resulting in methacrylates having generally higher T_gs than acrylates (*e.g.* T_g for PMMA is higher than 100 °C, while for PMA is about 10 °C).[45] The second aspect (*i.e.* physical entanglement), in particular for networks containing high levels of methacrylic cross-linker, might represent an important limit for the development of homogeneous scaffolds having randomly distributed cross-linking points. This is the case for systems polymerized by conventional FRP, as can be evidenced by comparing the porous structure in M100 with the one in A100. In the former case,

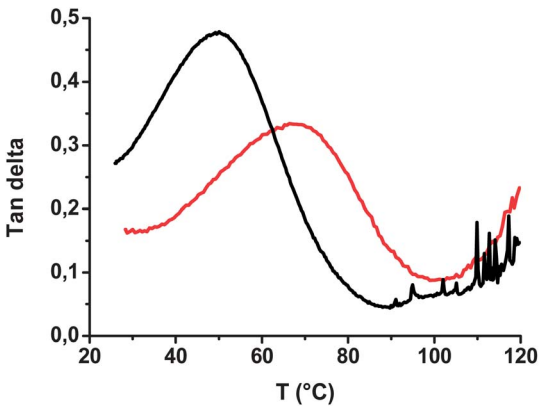

Fig. 4 Loss tangent (tan δ) *versus* temperature for A50 RAFT (red curve) and A50FRP (black curve).

phase separation occurs earlier, leading to a highly porous structure, although methacrylates polymerize more slowly than acrylates (thus favouring relaxation phenomena in the growing macroradicals), and toluene is a better solvent for methacrylates (based on the Hildebrand solubility parameters).[45] Interestingly, the use of RAFT can overcome this limit. If M100 RAFT has a considerably lower surface area compared to M100 FRP, this may be related to a delayed phase separation, as well as to an improved distribution of cross-linking points. However, if its surface area is even lower than that of A100 RAFT (for which entanglement phenomena on the polymer back-bone are less pronounced), this suggests that the ability of the methyl group to reduce the monomer reactivity largely compensates, for highly CL methacrylic RAFT polymers, the potential constraints generated by their stronger physical entanglement. To the best of our knowledge, this is the first time that such a comparison has been performed and extended to the molecular imprinting field.

Conclusions

In conclusion, we have synthesized and compared bulk acrylic and methacrylic polymers molecularly imprinted with the model compound *S*-propranolol, prepared by using two different radical polymerization approaches: free-radical polymerization and RAFT polymerization. For the first time, formulations containing progressively reduced amounts of cross-linker and based on two different classes of monomers (acrylic and methacrylic) were used in order to evaluate the effects of RAFT and FRP on MIPs. This allowed focusing on the properties of low cross-linked matrices, necessary for certain applications of MIPs. As a result, we have observed that RAFT is effective in generating higher affinity acrylic and methacrylic bulk MIPs compared to FRP. Upon reduction of the CL content from A/M100 up to A/M50, affinities were generally reduced, especially for acrylates. However RAFT allowed the maintenance of better template affinities compared to the corresponding FRP MIPs. In general, methacrylates perform better than acrylates in molecular imprinting, as they show considerably higher template affinities even when poorly cross-linked. From a structural point of view, RAFT has also shown to be effective in promoting the development of more homogeneous structures, containing improved distribution of the cross-linking points, as evidenced by SEM, BET, swelling, DMA and nanoindentation analyses. This aspect can in particular be associated with the controlled conditions induced by RAFT, wherein the propagating species coexist in the polymerization medium and they can more easily relax their structure during the growing step.

Acknowledgements

The authors thank Prof. Steven P. Armes from the University of Sheffield for access to the instrumentation for BET measurements, Dr Algi Serelis from DuluxGroup (previously from Orica Consumer Products) for the generous gift of the a-TTCA RAFT agent, the Physicochemical Analysis Group at Compiègne University of Technology for SEM images, and Dr Aude Cordin from Compiègne University of Technology for FT-IR analyses. C. Gonzato acknowledges the French Ministry for Research and Higher Education for providing his PhD fellowship. The authors acknowledge the European Regional Development Fund and the Regional Council of Picardie for co-funding of equipment under CPER 2007–2013.

Notes and references

1 R. Arshady and K. Mosbach, *Die Makromolekulare Chemie*, 1981, **182**, 687–692.
2 G. Wulff and A. Sarhan, *Angew. Chem., Int. Ed. Engl.*, 1972, **11**, 341–342.
3 G. Wulff, *Chem. Rev.*, 2002, **102**, 1–28.
4 K. Haupt, *Nat. Mater.*, 2010, **9**, 612–614.
5 K. Haupt, *Molecular Imprinting*, Springer, Heidelberg, 2012.
6 C. Alexander, H. S. Andersson, L. I. Andersson, R. J. Ansell, N. Kirsch, I. A. Nicholls, J. O'Mahony and M. J. Whitcombe, *J. Mol. Recognit.*, 2006, **19**, 106–180.
7 M. Bompart and K. Haupt, *Aust. J. Chem.*, 2009, **62**, 751–761.
8 C. J. Hawker, A. W. Bosman and E. Harth, *Chem. Rev.*, 2001, **101**, 3661–3688.
9 M. Kamigaito, T. Ando and M. Sawamoto, *Chem. Rev.*, 2001, **101**, 3689–3746.
10 K. Matyjaszewski and J. Xia, *Chem. Rev.*, 2001, **101**, 2921–2990.
11 J. Chiefari, Y. K. Chong, F. Ercole, J. Krstina, J. Jeffery, T. P. T. Le, R. T. A. Mayadunne, G. F. Meijs, C. L. Moad, G. Moad, E. Rizzardo and S. H. Thang, *Macromolecules*, 1998, **31**, 5559–5562.
12 J. Chiefari, R. T. A. Mayadunne, C. L. Moad, G. Moad, E. Rizzardo, A. Postma and S. H. Thang, *Macromolecules*, 2003, **36**, 2273–2283.
13 Y. K. Chong, J. Krstina, T. P. T. Le, G. Moad, A. Postma, E. Rizzardo and S. H. Thang, *Macromolecules*, 2003, **36**, 2256–2272.
14 P. Corpart, D. Charmot, T. Biadatti, S. Zard and D. Michelet, *WO Pat.* 1,998,058,974, 1998.
15 Y. Zhang and Z. Huiqi, *Chin. J. React. Polym.*, 2008, **17**, 1.
16 V. D. Salian and M. E. Byrne, *Macromol. Mater. Eng.*, 2013, **298**, 379–390.
17 B. Sellergren, B. Rückert and A. J. Hall, *Adv. Mater.*, 2002, **14**, 1204–1208.
18 C. Gonzato, M. Courty, P. Pasetto and K. Haupt, *Adv. Funct. Mater.*, 2011, **21**, 3947–3953.
19 G. Pan, Y. Ma, Y. Zhang, X. Guo, C. Li and H. Zhang, *Soft Matter*, 2011, **7**, 8428–8439.
20 L. Fang, S. Chen, X. Guo, Y. Zhang and H. Zhang, *Langmuir*, 2012, **28**, 9767–9777.
21 M. R. Halhalli, C. S. A. Aureliano, E. Schillinger, C. Sulitzky, M. M. Titirici and B. Sellergren, *Polym. Chem.*, 2012, **3**, 1033–1042.
22 N. Griffete, H. Li, A. Lamouri, C. Redeuilh, K. Chen, C. Z. Dong, S. Nowak, S. Ammar and C. Mangeney, *J. Mater. Chem.*, 2012, **22**, 1807–1811.
23 V. D. Salian, A. D. Vaughan and M. E. Byrne, *J. Mol. Recognit.*, 2012, **25**, 361–369.

24 A. D. Vaughan, S. P. Sizemore and M. E. Byrne, *Polymer*, 2007, **48**, 74–81.
25 A. D. Vaughan, J. B. Zhang and M. E. Byrne, *AIChE J.*, 2010, **56**, 268–279.
26 Y. Ma, G. Pan, Y. Zhang, X. Guo and H. Zhang, *J. Mol. Recognit.*, 2013, **26**, 240–251.
27 H. Gao, W. Li and K. Matyjaszewski, *Macromolecules*, 2008, **41**, 2335–2340.
28 T. Norisuye, T. Morinaga, Q. Tran-Cong-Miyata, A. Goto, T. Fukuda and M. Shibayama, *Polymer*, 2005, **46**, 1982–1994.
29 N. Sanson and J. Rieger, *Polym. Chem.*, 2010, **1**, 965–977.
30 A. R. Wang and S. Zhu, *Polym. Eng. Sci.*, 2005, **45**, 720–727.
31 Q. Yu, S. Xu, H. Zhang, Y. Ding and S. Zhu, *Polymer*, 2009, **50**, 3488–3494.
32 Q. Yu, Y. Zhu, Y. Ding and S. Zhu, *Macromol. Chem. Phys.*, 2008, **209**, 551–556.
33 J. Rosselgong, S. P. Armes, W. Barton and D. Price, *Macromolecules*, 2009, **42**, 5919–5924.
34 N. Griffete, H. Frederich, A. Maître, C. Schwob, S. Ravaine, B. Carbonnier, M. M. Chehimi and C. Mangeney, *J. Colloid Interface Sci.*, 2011, **364**, 18–23.
35 S. Li, R. Vatanparast and H. Lemmetyinen, *Polymer*, 2000, **41**, 5571–5576.
36 L. I. Andersson, *Anal. Chem.*, 1996, **68**, 111–117.
37 M. Bompart, L. A. Gheber, Y. De Wilde and K. Haupt, *Biosens. Bioelectron.*, 2009, **25**, 568–571.
38 R. J. Ansell and K. Mosbach, *Analyst*, 1998, **123**, 1611–1616.
39 C. Yu and K. Mosbach, *J. Chromatogr., A*, 2000, **888**, 63–72.
40 M. P. Stevens, *Polymer chemistry: an introduction*, Oxford University Press, New York, 1999.
41 E. S. Matsuo, M. Orkisz, S. T. Sun, Y. Li and T. Tanaka, *Macromolecules*, 1994, **27**, 6791–6796.
42 S. Sasaki, T. Ooya and T. Takeuchi, *Polym. Chem.*, 2010, **1**, 1684–1688.
43 N. Ide and T. Fukuda, *Macromolecules*, 1999, **32**, 95–99.
44 G. Odian, *Principles of polymerization*, John Wiley and Sons, Inc., Hoboken, New Jersey, 2004.
45 J. Brandrup, E. H. Immergut, E. A. Grulke, A. Abe and D. R. Bloch, *Polymer handbook*, John Wiley & Sons, Inc., 1999.

